Preprint typeset in JHEP style - PAPER VERSION DFTT 45/2009

Multiple Parton Interactions in $Z + 4j$, $W^{\pm}W^{\pm} + 0/2j$ and $W^{+}W^{-} + 2j$ production at the LHC

Ezio Maina[a,b]

[a] *INFN, Sezione di Torino, Italy,*
[b] *Dipartimento di Fisica Teorica, Università di Torino, Italy*

Abstract: The expected rate for Multiple Parton Interactions (MPI) at the LHC is large. This requires an estimate of their impact on all measurement foreseen at the LHC. Conversely it provides new means of studying MPI at the LHC. In this paper we examine the role of MPI at the LHC, with the design energy of 14 TeV, in

- Z production in association with four jets,
- $W^{\pm}W^{\pm}$ in association with zero or two jets.
- $W^{+}W^{-}$ in association with two jets.

In all cases the vector bosons are assumed to decay leptonically.
The MPI contribution to $Z + 4j$ is dominated by events with two jets with balancing transverse momentum. It is possible to achieve a good signal to background ratio, close to 20%, for MPI compared to Single Interaction processes by selecting events with two jets with large separation in the transverse plane. The corresponding statistical significance for a luminosity of 1 fb^{-1} is about 6.9 for the $\mu^{+}\mu^{-}$ channel alone.
The final state channel in which only two same–sign high transverse momentum charged leptons are required and additional hard jets are vetoed is dominated by MPI, with an expected yield of 2500 events with the full LHC luminosity.

Contents

1. Introduction **1**

2. Calculation **3**

3. Studying MPI in $Z + 4j$ processes **5**

4. Studying MPI in $W^{\pm}W^{\pm} + 0/2j$ processes **13**

5. MPI in $W^+W^- + 2j$ processes: a background to Higgs production via vector fusion in the $H \to WW \to \ell\ell\nu\nu$ channel? **16**

6. Conclusions **17**

A. A loose argument for the relative size of the effective cross sections in Double and Triple Parton Interactions **19**

1. Introduction

The presence of Multiple Parton Interactions (MPI) in high energy hadron collisions has been convincingly demonstrated [1, 2, 3].

MPI rates at the LHC are expected to be large, making it necessary to estimate their contribution to the background of interesting physics reactions. On the other hand, their abundance at the LHC makes it possible to study MPI experimentally in details, testing and validating the models which are used in the Monte Carlo's [4, 5, 6, 7] to describe these important features of hadron scattering. It is therefore of interest to search for new reactions in which MPI can be probed and to study in which kinematic regimes they are best investigated. Previous studies evaluated the MPI background to Higgs production in the channel $pp \to WH \to l\nu b\bar{b}$, [8], $4b$ production [9] and WH, ZH production [10]. Recently [11] the inclusive double dijet production has been discussed as a tool to gain information on the two–parton distribution in the proton. In Ref. [12, 13] it has been shown how the study of "inclusive" and "exclusive" multiple interaction cross sections can provide new information on the non–perturbative structure of the nucleon.

In [14] MPI have been studied as a background to top–antitop production at the LHC in the semileptonic channel, particularly in the early phase of data taking when the full power of b–tagging will not be available. In the same paper it has been shown that MPI can be accessed in the $W + 4j$ channel, a far more complicated setting than the reactions mentioned before and that the large cross section for two jet production makes it possible to detect Triple Parton Interactions (TPI) in $W + 4j$ production.

Different reactions involve different combinations of initial state partons, for instance γ+3j, Z+3j, W+3j MPI processes test specific sets of quark and gluon distributions inside the proton. The comparison of several MPI processes will also allow to study the possible x–dependence of these phenomena, namely the dependence on the fraction of momentum carried by the partons. CDF found no evidence of x–dependence in their data which included jets of transverse momentum as low as five GeV. However in Ref.[15, 16, 17] it was shown that correlations between the value of the double distribution functions for different values of the two momentum fractions x_1, x_2 are to be expected, even under the assumption of no correlation at some scale μ_0, as a consequence of the evolution of the distribution functions to a different scale μ, which is determined by an equation analogous to the usual DGLAP equation. In [17] the corrections to the factorized form for the double distribution functions have been estimated. They depend on the factorization scale, being larger at larger scales Q, and on the x range, again being more important at larger momentum fractions. For $Q = M_W$ and $x \sim 0.1$ the corrections are about 35% for the gluon-gluon case. Moreover Ref.[17] showed that the correlations in x_1, x_2 space are different for different pairs of partons, pointing to an unavoidable flavour dependence of the double distribution functions.

In this paper we examine

- the background generated by MPI to $Z + 4j \to \ell^+\ell^- + 4j$ production and the possibility of studying MPI in the $Z + 4j$ channel.
- the observability of MPI in the $W^\pm W^\pm \to \ell^\pm \ell'^\pm$ channel.
- the background generated by MPI to $W^+W^- + 2j$ production and therefore to Higgs production via vector fusion in the $H \to WW \to \ell\ell\nu\nu$ channel

at the LHC, with the design energy of 14 TeV.

With its five final state particles, $Z + 4j$ production gives the opportunity to study MPI in a more complex final state than in most previous analysis which have typically involved a combination of two $2 \to 2$ processes. The cross section for $Z + 4j$ production is expected to be smaller than the cross section for $W + 4j$, mainly because of the smaller branching ratio to charged leptons in the first case. However the $Z + 4j$ channel is cleaner from an experimental point of view than the $W + 4j$ one since isolated, high pT charged leptons which are the hallmark of W detection can be copiously produced in B-hadron decays [18] while no comparable mechanism exists for generating lepton pairs of mass in the M_Z region.

The large expected cross section for two jet production suggests that also Triple Parton Interactions (TPI) could provide a non negligible contribution in this channel, as shown to be the case for $W + 4j$ processes.

The $W^\pm W^\pm$ final state has the unique feature that it can be produced through MPI at a lower perturbative order, $\mathcal{O}(\alpha_{EM}^4)$ including W decays, than in Single Parton Interactions (SPI) which start at $\mathcal{O}(\alpha_{EM}^6)$ and $\mathcal{O}(\alpha_{EM}^4 \alpha_S^2)$ with two additional quarks in the final state. This peculiarity has been noticed before in Ref. [19], which studied the inclusive production of two same–sign stable W's at the LHC. Later additional results concerning the effects of

parton correlations have appeared in the literature[17]. Here we treat separately the case in which the two additional jets are actually observed and the case in which no jet is required to be present in the final state. In the first case we will consider all processes contributing to $W^{\pm}W^{\pm} + 2j$. In the second case two different approaches can be adopted: on one hand the inclusive production of two same–sign W's plus any additional jet activity can be studied, on the other hand the focus can be brought to the more exclusive production of two same–sign W's and no observable jet. In the latter case a jet threshold is selected and a jet veto is applied: no event with a jet above threshold is accepted.

The $W^+W^- + 2j$ channel is one of the most important channels for Higgs discovery over a large portion of the allowed range for the Higgs mass within the SM [20, 21] and an estimate of MPI for this final state is definitely in order.

In Sect. 2 the main features of the calculation are discussed. Then we present our results in Sect. 3–5. Finally we summarize the main points of our discussion.

2. Calculation

The MPI processes which contribute to $Z + 4j$ through Double Parton Interactions (DPI) are

- $jj \otimes jjZ$
- $jjj \otimes jZ$
- $jjjj \otimes Z$.

For opposite sign W's in $WW + 2j$ they are

- $jj \otimes WW$
- $jW \otimes jW$
- $jjW \otimes W$

while for equal sign W's in $WW + 2j$ the relevant pairs are

- $jW \otimes jW$
- $jjW \otimes W$

where the symbol $\otimes$ stands for the combination of one event for each of the two final states it connects.

The cross section for DPI has been estimated as

$$\sigma = \sigma_1 \cdot \sigma_2 / \sigma_{eff} \tag{2.1}$$

where σ_1, σ_2 are the cross sections of the two contributing reactions. At the Tevatron, CDF [2] has measured $\sigma_{eff} = 14.5 \pm 1.7^{+1.7}_{-2.3}$ mb, a value confirmed by D0 which quotes $\sigma_{eff} =$

15.1 ± 1.9 mb [3]. In Ref.[22] it is argued, on the basis of the simplest two channel eikonal model for the proton–proton cross section, that a more appropriate value at $\sqrt{s} = 1.8$ TeV is 10 mb which translates at the LHC into $\sigma_{eff}^{LHC} = 12$ mb. Treleani then estimates the effect of the removal by CDF of TPI events from their sample and concludes that CDF measurement yields $\sigma_{eff} \approx 11$ mb. In the following we conservatively use $\sigma_{eff} = 14.5$ mb with the understanding that this value is affected by an experimental uncertainty of about 15% and that it agrees only within 30% with the predictions of the eikonal model. Since σ_{eff} appears as an overall factor in our results it is easy to take into account the smaller value advocated in [22].

The only TPI process contributing to $Z + 4j$ is

- $jj \otimes jj \otimes Z$.

while the corresponding reaction for $WWjj$, both for opposite and for equal sign W's production is

- $jj \otimes W \otimes W$.

The cross section for TPI, under the same hypotheses which lead to Eq.(2.1), can be expressed as:

$$\sigma = \sigma_1 \cdot \sigma_2 \cdot \sigma_3 / \left(\sigma_{3,eff}\right)^2 / k \tag{2.2}$$

where k is a symmetry factor. $\sigma_{3,eff}$ has not been measured, and in principle it could be different from σ_{eff}. However, in the absence of actual data, we will assume $\sigma_{3,eff} = \sigma_{eff}$. In Appendix A we present a non rigorous argument which supports the fact that the two effective cross sections are indeed comparable. In the following we will keep the TPI contributions, which are affected by larger uncertainties, separated from the DPI predictions which are based on firmer ground.

Three perturbative orders contribute to $4j + \ell^{\pm}\ell^{\mp}$ at the LHC through Single Parton Interactions, while two perturbative orders contribute to $\ell\ell'\nu\nu + 2j$. The $\mathcal{O}(\alpha_{EM}^6)$ and $\mathcal{O}(\alpha_{EM}^4 \alpha_S^2)$ samples have been generated with `PHANTOM` [23, 24, 25], while the $\mathcal{O}(\alpha_{EM}^2 \alpha_S^4)$ sample has been produced with `MADEVENT` [26]. All reactions contributing to MPI have been generated with `MADEVENT`. Both programs generate events in the Les Houches Accord File Format [27]. In all samples full matrix elements, without any production times decay approximation, have been used. All samples have been generated using CTEQ5L [28] parton distribution functions.

The relatively high transverse momentum threshold, $p_{T_j} > 30$ GeV, and mass separation, $M_{jj} > 60$ GeV, we have adopted for all reactions with jets in the final state ensures that the processes we are interested in can be described by (fixed order) perturbative QCD.

For the $\mathcal{O}(\alpha_{EM}^6)$ and $\mathcal{O}(\alpha_{EM}^4 \alpha_S^2)$ samples, generated with `PHANTOM`, the QCD scale (both in α_s and in the parton distribution functions) has been taken as

$$Q^2 = M_W^2 + \frac{1}{6} \sum_{i=1}^{6} p_{Ti}^2. \tag{2.3}$$

For the $\mathcal{O}(\alpha_{EM}^2\alpha_S^4)$ sample the scale has been set to $Q^2 = M_Z^2$. This difference in the scales leads to a definite relative enhancement of the $4j + Z$ SPI background and of the MPI contribution compared to the other ones. Tests in comparable reactions have shown an increase of about a factor of 1.5 for the processes computed at $Q^2 = M_Z^2$ with respect to the same processes computed with the larger scale Eq.(2.3). This is the level of uncertainty which is expected for all the results presented in this paper from variations of the QCD scale. This estimate is confirmed by the results shown in Ref.[29, 30] where the NLO cross section for the comparable reaction $W + 3j$ has been computed and confronted with the LO result. Other uncertainties stem from the neglect of correlations in the two–particle distribution functions which, as mentioned in the Introduction, can be as large as 40% and from the experimental and theoretical uncertainties on σ_{eff} which range between 15% and 30%. Therefore we expect our prediction to be correct within a factor of about two.

In order to produce the Multiple Parton Interaction samples we have combined at random one event from each of the reactions which together produce the desired final state through MPI. When needed, we have required that each pair of colored partons in the final state have a minimum invariant mass. This implies that the combined cross section does not in general correspond to the product of the separate cross sections divided by the appropriate power of σ_{eff} because the requirement of a minimum invariant mass for all jet pairs induces a reduction of the cross section when additional pairs are formed in superimposing events.

We work at parton level with no showering and hadronization. Color correlations between the two scatterings have been ignored. They are known to be important at particle level [31] but are totally irrelevant at the generator level we are considering in this paper.

3. Studying MPI in $Z + 4j$ processes

This reaction shows strong similarities to the $W + 4j$ channel studied in [14]. In both cases we are dealing with a five body final state and the MPI cross section is dominated by the $jj \otimes jjV$ mechanism. $Z + 4j$ rates are smaller than $W + 4j$ but the first reaction is somewhat cleaner from an experimental point of view since leptonically decaying Z can be detected without ambiguities exploiting the high expected precision for lepton pair masses and are essentially free of background.

In our estimates below we have only taken into account the muon decay of the Z boson. The $Z \to e^+e^-$ channel gives the same result. The possibility of detecting high p_T taus has been extensively studied in connection with the discovery of a light Higgs in Vector Boson Fusion in the $\tau^+\tau^-$ channel [32] with extremely encouraging results. Efficiencies of order 50% have been obtained for the hadronic decays of the $\tau's$. The expected number of events in the $H \to \tau\tau \to e\mu + X$ is within a factor of two of the yield from $H \to WW^* \to e\mu + X$ for $M_H = 120$ GeV where the $\tau\tau$ and WW^* branching ratios of the Higgs boson are very close, suggesting that also in the leptonic decay channels of the taus the efficiency is quite high. Therefore we expect the $Z \to \tau^+\tau^-$ channel to increase the detectability of the $Z+4j$ final state.

Process	Cross section	Combined
jj	1.4×10^8 pb	3.8×10^2 fb
$jj\mu^+\mu^-$	61 pb	
jjj	7.6×10^6 pb	62 fb
$j\mu^+\mu^-$	1.7×10^2 pb	
$jjjj$	1.2×10^6 pb	75 fb
$\mu^+\mu^-$	9.3×10^2 pb	

Table 1: Cross sections for the processes which contribute to $4j + \ell^+\ell^-$ through DPI. The selection cuts are given in Eq.(3.1). Notice that the combined cross section corresponds to $\sigma_1 \cdot \sigma_2/\sigma_{eff}$ only for the $jjjj \otimes Z$ case. In all other cases there is a reduction due to the requirement of a minimum invariant mass for all jet pairs since additional pairs are formed when the two events are superimposed.

Process	Cross section	Combined
jj	1.4×10^8 pb	23 fb
jj	1.4×10^8 pb	
$\mu^+\mu^-$	9.3×10^2 pb	

Table 2: Cross sections for the processes which contribute to $4j + \ell^+\ell^-$ through TPI. The selection cuts are given in Eq.(3.1).

The two jets with the largest and smallest rapidity are identified as forward and backward jet respectively. The two intermediate jets will be referred to as central jets in the following.

All samples have been generated with the following cuts:

$$\begin{aligned} p_{T_j} &\geq 30 \text{ GeV}\,, \quad |\eta_j| \leq 5.0\,, \\ p_{T_\ell} &\geq 20 \text{ GeV}\,, \quad |\eta_\ell| \leq 3.0\,, \\ M_{jj} &\geq 60\,\text{GeV}\,, \quad M_{ll} \geq 20\,\text{GeV} \end{aligned} \tag{3.1}$$

where $j = u, \bar{u}, d, \bar{d}, s, \bar{s}, c, \bar{c}, b, \bar{b}, g$.

The cross sections for the reactions which enter the MPI sample are shown in Tab.1 and Tab.2 for DPI and TPI respectively. The largest contribution is given by processes in which the Z boson is produced in association with two jets in one interaction and other two jets are produced in the second one. As a consequence, as in the case of $\gamma + 3j$ studied by CDF [2] and of the $W + 4j$ channel most of the events contain a pair of energetic jets with balancing transverse momentum. The next largest contribution is due to Drell-Yan processes combined with four jet events. The smallest, but still sizable, DPI contribution is given by processes in which the Z boson is produced in association with one jet, which

Process	Cross section	Cross section	Cross section	Cross section
$\mathcal{O}(\alpha_{EM}^4\alpha_S^2)$	1.1×10^2 fb	88 fb	26 fb	17 fb
$\mathcal{O}(\alpha_{EM}^2\alpha_S^4)$	6.4×10^3 fb	5.6×10^3 fb	2.2×10^3 fb	1.4×10^3 fb
$\mathcal{O}(\alpha_{EM}^2\alpha_S^4)_{\rm DPI}$	5.2×10^2 fb	4.7×10^2 fb	2.7×10^2 fb	2.5×10^2 fb
$\mathcal{O}(\alpha_{EM}^2\alpha_S^4)_{\rm TPI}$	23 fb	21 fb	15 fb	15 fb
$\mathcal{O}(\alpha_{EM}^6)$	17 fb	14 fb	7.6 fb	4.8 fb

Table 3: Cross sections for the processes which contribute to $4j + \mu^+\mu^-$. For the second column the selection cuts are given in Eq.(3.1). For the third column the additional isolation requirement Eq.(3.2) has been applied. The events entering the fourth column also satisfy the condition Eq.(3.3) on the separation between the most forward and most backward jets. Finally in the last column we present the cross section obtained considering only events for which the largest azimuthal angular separation satisfies Eq.(3.4).

balances the Z transverse momentum, and the other three jets are produced in the second interaction. The cross section for TPI is 23 fb, about 5% of all MPI processes.

The cross section for Single Particle Interaction processes and Multiple Parton Interactions contributing to the $jjjj\mu^+\mu^-$ final state, with the set of cuts in Eq.(3.1), are shown in the second column of Tab. 3. The cross sections in the third column have been obtained with the additional requirements:

$$\Delta R(jj) > 0.5 \qquad \Delta R(jl^{\pm}) > 0.5 \tag{3.2}$$

which ensure that all jet pairs are well separated and that the charged leptons are isolated from jets.

Fig. 1 shows that MPI events tend to have larger separation in pseudorapidity between the most forward and most backward jets than $Z + 4j$ at $\mathcal{O}(\alpha_{EM}^2\alpha_S^4)$ which is the only significant background.

Therefore we further require:

$$|\Delta\eta(j_f j_b)| > 3.8 \tag{3.3}$$

In a more realistic environment in which additional jets generated by showering cannot be ignored, one could impose condition (3.3) on the most forward and most backward of the four most energetic jets in the event.

The corresponding results are given in the fourth column of Tab. 3. Assuming a luminosity of 1 fb^{-1} this corresponds to a statistical significance of the MPI $4j + \mu^+\mu^-$ signal of about 6.1 if we take into account both the DPI and TPI contributions, and of 5.8 if we conservatively consider only DPI processes.

Fig. 2 presents the distribution on the invariant mass of the four jet plus charged leptons system. It shows that typically MPI events are less energetic than all other contributions considered in this paper.

In Fig. 3 we present the distribution of the largest $\Delta\phi$ separation between all jet pairs. Fig. 3 confirms that MPI processes leading to $Z + 4j$ events are characterized by the

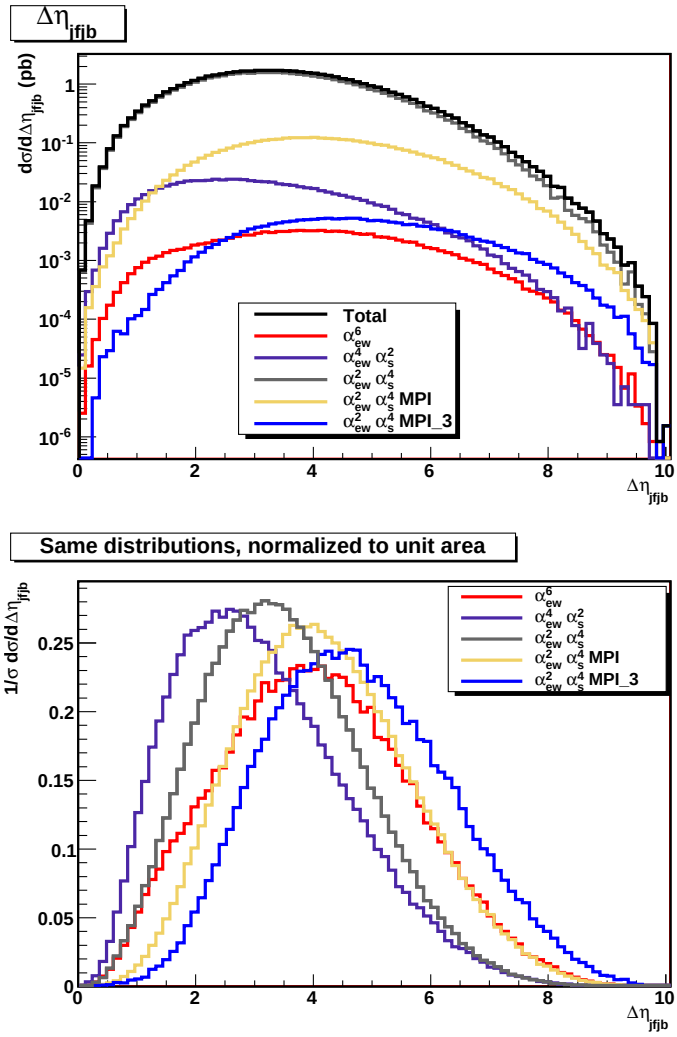

Figure 1:

$\Delta\eta$ separation between the most forward and most backward jet for the different contributions and for their sum. Cuts as in Eq.(3.1) and Eq.(3.2). The curves in the lower plot are normalized to unit area.

presence of two jets which are back to back in the transverse plane. The $Z+4j$ $\mathcal{O}(\alpha_{EM}^2\alpha_S^4)$ SPI contribution displays a much milder increase in the back to back region. All other contributions are negligible.

The expected $\Delta\phi$ resolution is of the order of a few degrees for both ATLAS [20] and CMS [21] for jets with transverse energy above 50 GeV. This resolution is comparable to the width of the bins in Fig. 3. We have examined the $\Delta\phi$ separation among pairs of jets ordered in energy, $E_{j_i} > E_{j_{i+1}}$. No clear pattern has emerged. In Fig. 4 we show the $\Delta\phi$ separation between the two most energetic jets, on the left, and of the two least energetic ones, on the right. As might have been guessed by the total mass distribution in Fig. 2 the

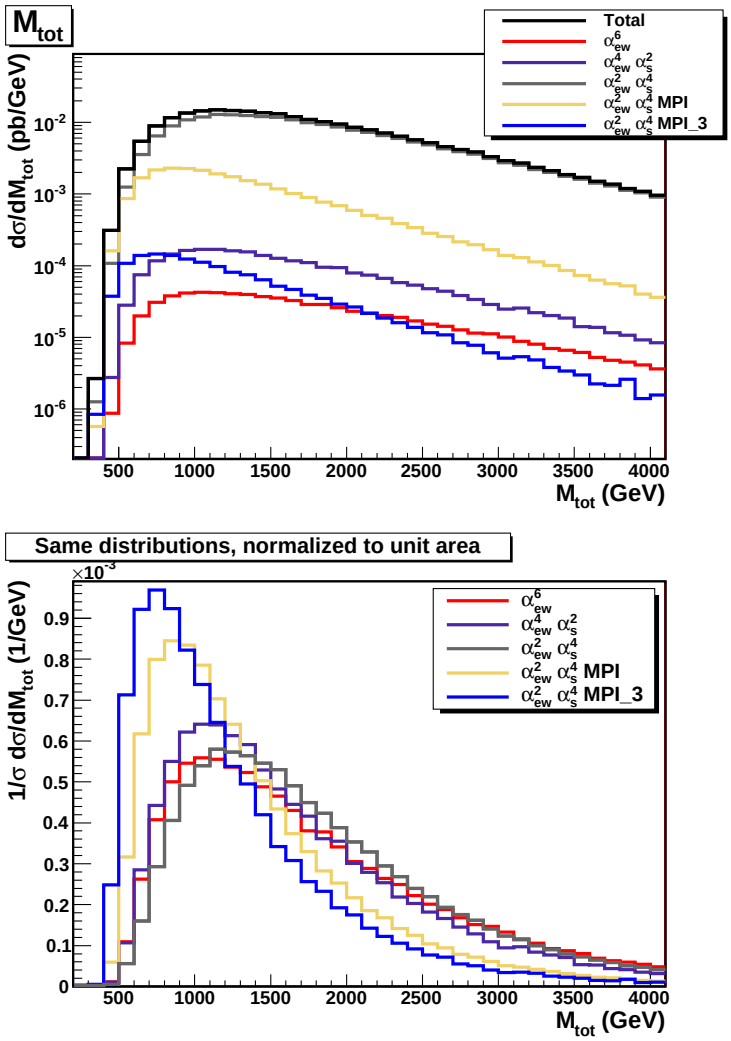

Figure 2: Distribution of the total invariant mass of the events for the different contributions and for their sum. Cuts as in Eq.(3.1), Eq.(3.2) and Eq.(3.3). The curves in the lower plot are normalized to unit area.

ratio between the MPI signal at $\Delta\phi = \pi$ and the $Z + 4j$ background is somewhat larger for softer jet pairs than for harder ones. It has proved impossible to clearly associate the two balancing jets with either the most forward/backward pair or with the central jets.

We can restrict our attention to the events for which the maximum $\Delta\phi$ among jets is in the interval:

$$|\Delta\phi(jj)_{max}| > 0.9 \cdot \pi \tag{3.4}$$

The corresponding cross sections are shown in the last column of Tab. 3. The rate decrease is of the order of 30% for Single Parton Interactions and essentially negligible for MPI processes.

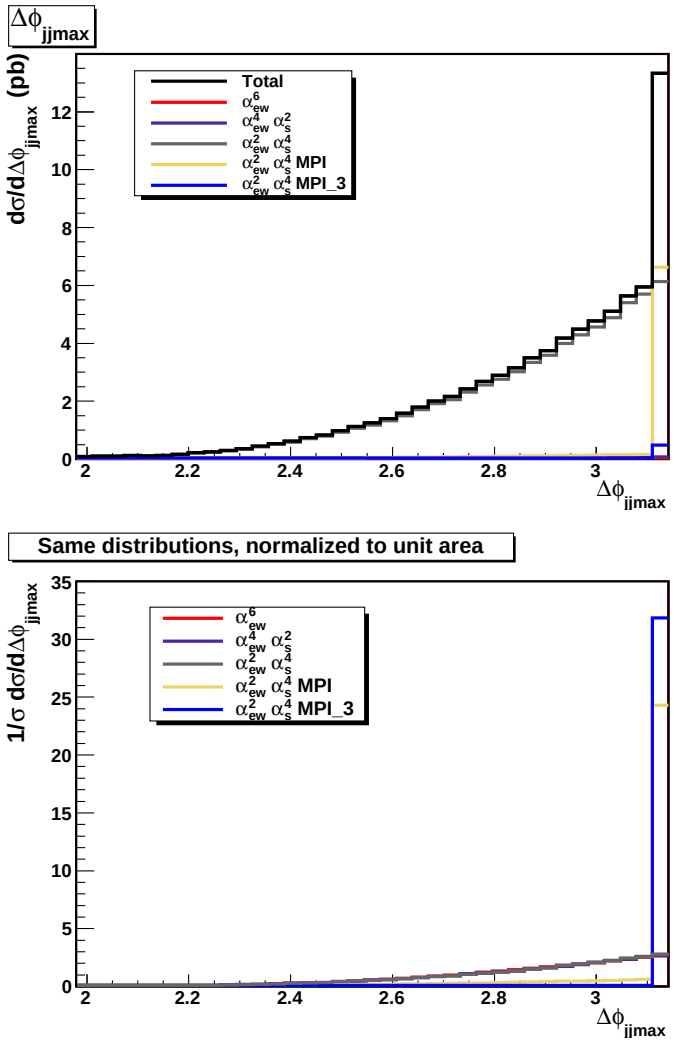

Figure 3: Largest $\Delta\phi$ separation between jet pairs for the different contributions and for their sum. Cuts as in Eq.(3.1), Eq.(3.2) and Eq.(3.3). The curves in the lower plot are normalized to unit area.

It appears quite feasible to achieve a good signal to background ratio, close to 18/100, for Multiple Interactions Processes compared to Single Interaction ones by selecting events with two jets with large separation in the transverse plane. The corresponding statistical significance for a a luminosity of 1 fb^{-1} is about 6.9 for the $\mu^+\mu^-$ channel alone with 260/1430 signal/background events. Figs. 3, 4 show that the SPI background is smooth in the region $|\Delta\phi(jj)_{max}| \sim \pi$ and almost flat for azimuthal angular differences among energy–ordered jets while the MPI signal is mostly concentrated at $|\Delta\phi| \sim \pi$. This opens the possibility of measuring the Single Parton Interaction contribution from the neighboring bins decreasing drastically all theoretical uncertainties on the evaluation of the background. By measuring ratios of observed events in nearby bins most of the experimental uncertainties will also cancel.

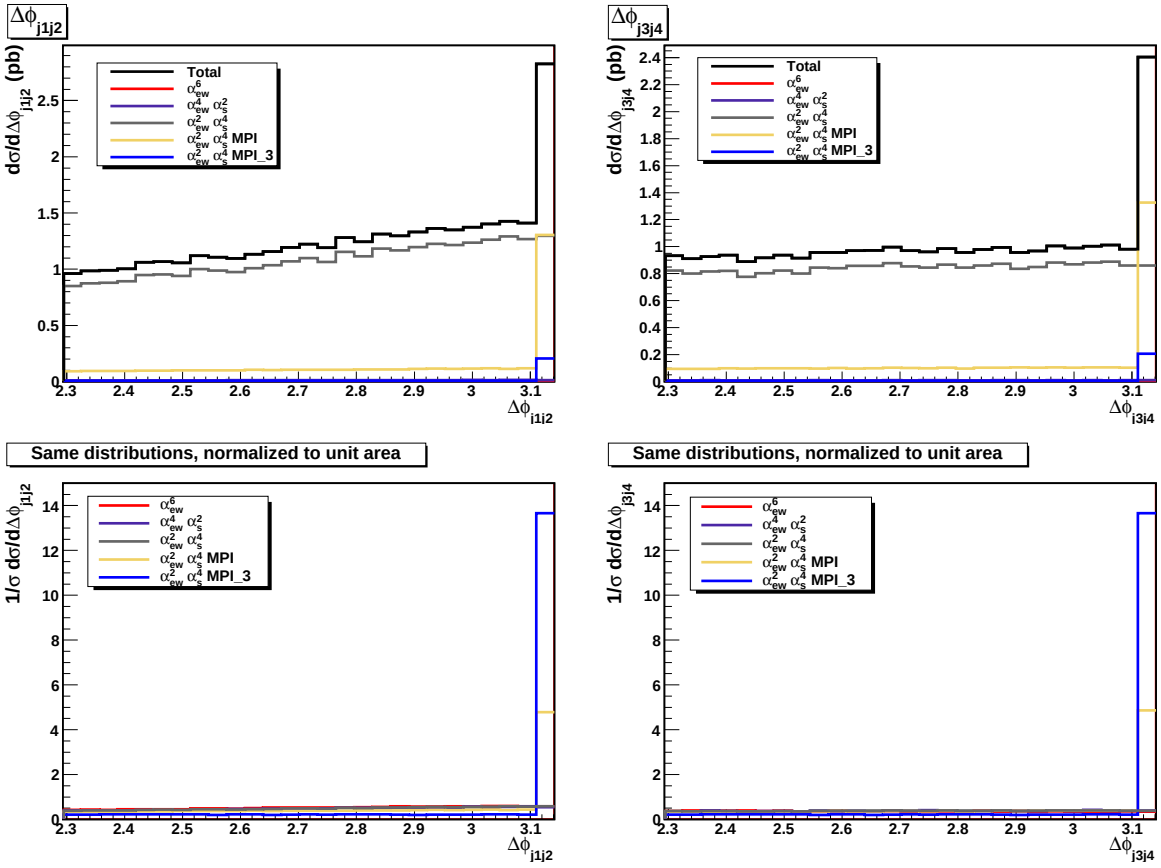

Figure 4: $\Delta\phi$ separation between the two most energetic jets (on the left) and between the two least energetic among the four jets (on the right) for the different contributions and for their sum. Cuts as in Eq.(3.1), Eq.(3.2) and Eq.(3.3). The curves in the lower plot are normalized to unit area.

Let us now turn to Triple Parton Interactions in more detail. The obvious traits which characterize these events are the presence of two pairs of jets which balance in transverse momentum and of one Z produced by a Drell-Yan interaction which, to lowest order, has zero the transverse momentum. While the first feature is not typically found in DPI, Z bosons of Drell-Yan origin are present in $jjjj \otimes Z$ events which account for about 15% of DPI. This is illustrated in Fig. 5 and Fig. 6. For these two plots we have only considered events satisfying all constraints in Eq.(3.1), Eq.(3.2), Eq.(3.3) and Eq.(3.4).

Fig. 5 shows the angular separation in the transverse plane, $\Delta\phi_{comp}$, between the two jets which do not belong to the pair with the largest $\Delta\phi$ in the event. The TPI contribution is concentrated at $\Delta\phi_{comp} \sim \pi$ while all other distributions are rather flat in that region. With the normalization $\sigma_{3,eff} = \sigma_{eff}$ in Eq.(2.2), TPI give the largest contribution in the bin at $\Delta\phi_{comp} = \pi$, amounting to more than 50% of the total.

Fig. 6 presents the distribution of the total transverse momentum of the charged lepton pair; it suggests that the presence of two charged lepton with essentially zero transverse momentum is of limited use in separating TPI events from their background.

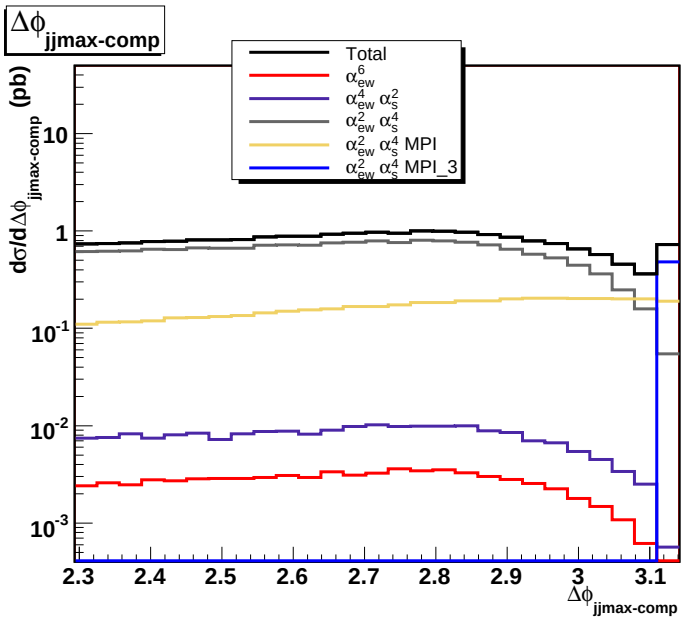

Figure 5: $\Delta\phi$ separation between the two jets which do not belong to the pair with the largest $\Delta\phi$ in the event. Cuts as in Eq.(3.1), Eq.(3.2), Eq.(3.3) and Eq.(3.4).

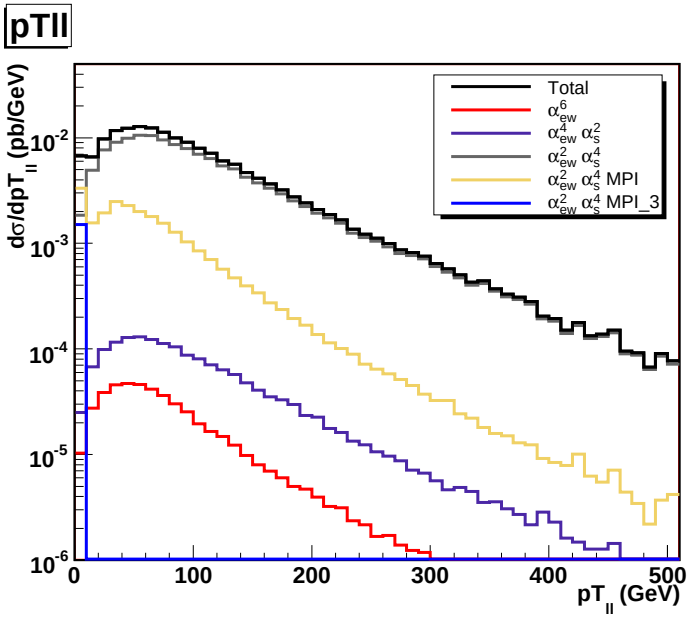

Figure 6: Distribution of the transverse momentum of the l^+l^- system. Cuts as in Eq.(3.1), Eq.(3.2), Eq.(3.3) and Eq.(3.4).

The rates for TPI at the LHC are sizable. Even at low luminosity, L = 30 fb^{-1}/year, about 450 TPI events per year are expected for each charged lepton type. The corresponding background, integrating over the region $\Delta\phi_{comp} > 0.9\pi$, yields about 7500 events

leading to a promising statistical significance larger than five. Because of the lack of information concerning the rate of Triple Parton Interactions, it is impossible to draw any firm conclusion from our preliminary analysis; Fig. 5 however suggests that indeed it might well be possible to investigate TPI at the LHC exploiting the angular distribution of pairs of jets with the standard total luminosity expected at the LHC of about 300 fb^{-1} despite the uncertainties which affect the prediction.

4. Studying MPI in $W^{\pm}W^{\pm} + 0/2j$ processes

As mentioned in the introduction $W^{\pm}W^{\pm}$ production has the peculiarity that while the SPI contribution starts at $\mathcal{O}(\alpha_{EM}^6)$ and $\mathcal{O}(\alpha_{EM}^4\alpha_S^2)$, the MPI mechanism can produce two same–sign highly isolated leptons at $\mathcal{O}(\alpha_{EM}^4)$ if no additional jets are required in the final state.

$W^{\pm}W^{\pm}+2j$ production has been shown [33] to be the vector–vector scattering reaction which is most sensitive to the details of the EWSB mechanism, which can be studied in first approximation comparing cross sections calculated in the presence of a light Higgs and with the Higgs mass taken to infinity. Unfortunately the expected rate is small and this channel has to contend with the contribution to isolated lepton production coming from B-hadron decays [18].

The inclusive production of same–sign stable W's has been studied in Ref.[19], which included all $\mathcal{O}(\alpha_{EM}^4)$ and $\mathcal{O}(\alpha_{EM}^2\alpha_S^2)$ contributions without taking into account W decays. In Ref. [17] the effects in this channel of the correlated evolution of double parton densities have been studied. While we ignore this issue in the present analysis, we take into account the decay of the W bosons and require an experimentally reasonable minimum transverse momentum for the charged leptons. We also estimate the background due to SM production of same–sign W's through SPI at $\mathcal{O}(\alpha_{EM}^6)$ and $\mathcal{O}(\alpha_{EM}^4\alpha_S^2)$, including again W decays.

For $W^{\pm}W^{\pm} + 2j$ processes the set of MPI reactions to be included is the full list mentioned in Sect. 2. The corresponding samples have been generated with the set of cuts shown below:

$$\begin{aligned} p_{T_j} &\geq 30 \text{ GeV}\,, \quad |\eta_j| \leq 5.0\,, \\ p_{T_\ell} &\geq 20 \text{ GeV}\,, \quad |\eta_\ell| \leq 3.0\,, \\ M_{jj} &\geq 60\,\text{GeV}. \end{aligned} \tag{4.1}$$

If, on the contrary, one aims to reveal MPI production and considers SPI as a a background then one can resort to a jet veto in order to suppress the SM SPI contribution. In this case only the $W \otimes W$ channel has to be considered in generating the signal. The additional MPI contributions entering $WW + 2j$ production are here part of higher order corrections and should be combined with the appropriate virtual contributions in order to obtain a finite correction. It is perhaps worth pointing out that the $\mathcal{O}(\alpha_{EM}^6)$ and $\mathcal{O}(\alpha_{EM}^4\alpha_S^2)$ SPI matrix element squared can be integrated over the full phase space without encountering any soft or collinear singularity. Therefore, the $\mathcal{O}(\alpha_{EM}^6)$ and $\mathcal{O}(\alpha_{EM}^4\alpha_S^2)$ sample used

for the zero–j analysis in this section has been generated without any constraint on the final state quarks. The charged leptons are required to satisfy the standard requirements:

$$p_{T_\ell} \geq 20 \text{ GeV}\,, \quad |\eta_\ell| \leq 3.0\,. \tag{4.2}$$

while no condition is imposed on their combined mass.

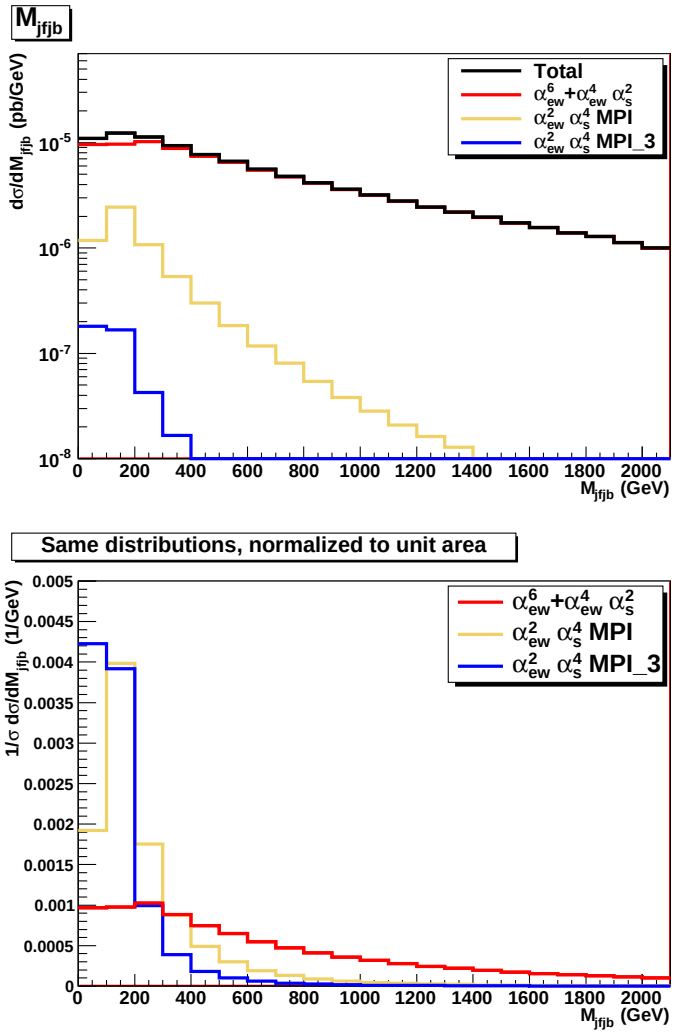

Figure 7: Distribution of the invariant mass of the two tag jets in $W^\pm W^\pm + 2j$ events. Cuts as in Eq.(4.1). The curves in the lower plot are normalized to unit area.

We will discuss first the case in which two jets are detected in the final state in addition to a same–sign lepton pair. Fig. 7 presents the mass distribution of the two tag jets. It shows that MPI events are concentrated at small invariant masses while the SPI spectrum extends to very large invariant masses. Therefore one can improve the statistical significance of the MPI signal requiring:

$$M_{j_f j_b} \leq 300 \text{ GeV}. \tag{4.3}$$

The cross sections before and after the application of the cut in Eq.(4.3) are given in the second and third column of Tab. 4 respectively for the $e^{\pm}\mu^{\pm}$ channel which is half of the total same-sign lepton sample.

Process	Cross section	Cross section
$\mathcal{O}(\alpha_{EM}^6)$+$\mathcal{O}(\alpha_{EM}^4\alpha_S^2)$	10 fb	3.0 fb
$\mathcal{O}(\alpha_{EM}^4\alpha_S^2)_{\rm DPI}$	0.6 fb	0.5 fb
$\mathcal{O}(\alpha_{EM}^4\alpha_S^2)_{\rm TPI}$	0.04 fb	0.04 fb

Table 4: Cross sections for the processes which contribute to $W^{\pm}W^{\pm}+2j$ in the $e\mu$ channel. For the second column the selection cuts are given in Eq.(4.1). For the third column the additional requirement Eq.(4.3) has been applied.

For a luminosity of 300 fb^{-1}, which is roughly the total expected luminosity at the LHC, and taking into account all possible decay channels to same–sign muons and electrons the statistical significance of the MPI signal is 6.7 and the expected number of signal/background events is 280/1780 per experiment. Clearly focusing on relatively soft tag jets makes this result more sensitive to the presence of additional jets from parton showering.

The final state channel in which only two same–sign high transverse momentum charged leptons are required has a much larger rate. In the first column of Table 5 the total cross section with the cuts in Eq.(4.2) are presented, while in the second column we show the results requiring that no jet with $p_{T_j} \geq 30$ GeV appears in the event. The ratio between MPI and SPI rates without any jet veto is about 1/3. The corresponding totally inclusive result presented in Ref. [19] is appreciably larger, close to 1/2. This difference is due to our cuts on the charged lepton transverse momentum and pseudorapidity Eq.(4.2) which are more easily satisfied when the two W's are produced in association with two extra jets and therefore with a non-zero transverse momentum.

Process	Cross section	Cross section
$\mathcal{O}(\alpha_{EM}^6)$+$\mathcal{O}(\alpha_{EM}^4\alpha_S^2)$	14 fb	0.9 fb
$\mathcal{O}(\alpha_{EM}^4)_{\rm DPI}$	4.3 fb	4.3 fb

Table 5: Cross sections for the processes which contribute to $W^{\pm}W^{\pm}+0j$ in the $e\mu$ channel. The selection cuts are given in Eq.(4.2). The results in the last column have been obtained vetoing jets with $p_{T_j} \geq 30$ GeV.

One sees that only a small fraction of the $\mathcal{O}(\alpha_{EM}^6)$+$\mathcal{O}(\alpha_{EM}^4\alpha_S^2)$ events have no hard jet in the final state and therefore the background is reduced to only about 20% of the signal. In the presence of a jet veto the cross section for the production of two same–sign

leptons is dominated by MPI. The expected rate for all possible combinations of same–sign leptons is about 2500 events per experiment for a luminosity of 300 fb^{-1}. Therefore the $\mathcal{O}(\alpha_{EM}^6)+\mathcal{O}(\alpha_{EM}^4\alpha_S^2)$ background is of little concern. In this case the real issue are jets faking isolated leptons and the actual isolated leptons from B-hadrons which require a detailed simulation far beyond the crude estimates presented here.

5. MPI in $W^+W^- + 2j$ processes: a background to Higgs production via vector fusion in the $H \to WW \to \ell\ell\nu\nu$ channel?

Higgs production in vector boson fusion followed by the decay of the Higgs to a W pair which in turn decays to two opposite charge leptons and two neutrinos is arguably the best channel for Higgs discovery over a large portion of the allowed range for the Higgs mass within the SM [20, 21]. In this case no Higgs peak is present in the data, and more refined analysis are needed. The main background in this channel is top-antitop production, possibly in association with jets. In the following we estimate the background provided by $W^+W^- + 2j$ through DPI. The $\mathcal{O}(\alpha_{EM}^4\alpha_S^2)$ sample includes top-antitop production but misses all $t\bar{t}$+*jets* processes and as a consequence underestimates the $t\bar{t}$ overall contribution. This is however sufficient since our conclusion is that the DPI $W^+W^- + 2j$ background is overwhelmed by $t\bar{t}$ production. We roughly follow the analysis scheme presented in [34]. The contribution from processes in which all external particles are fermions ($8f$), which includes Higgs production as well as all $q\overline{q} \to t\bar{t}$ processes, has been kept separated from the contribution with two external gluons ($2g6f$), which is completely dominated by top-antitop production. All samples have been generated with the following set of cuts:

$$\begin{aligned} p_{T_j} &\geq 30 \text{ GeV}\,, \quad |\eta_j| \leq 5.0\,, \\ p_{T_\ell} &\geq 20 \text{ GeV}\,, \quad |\eta_\ell| \leq 3.0\,, \\ M_{jj} &\geq 100\,\text{GeV}\,, \quad M_{ll} \geq 20\,\text{GeV} \end{aligned} \tag{5.1}$$

The corresponding cross sections are presented in the second column of Table 6.

Process	Cross section	Cross section	Cross section
$\mathcal{O}(\alpha_{EM}^6) + \mathcal{O}(\alpha_{EM}^4\alpha_S^2)$ $8f$	9.6×10^2 (2.5) fb	14 (1.0) fb	12 (0.9) fb
$\mathcal{O}(\alpha_{EM}^4\alpha_S^2)$ $2g6f$	6.0×10^3 fb	26 fb	16 fb
$\mathcal{O}(\alpha_{EM}^4\alpha_S^2)_{\text{DPI}}$	5.8 fb	0.09 fb	0.06 fb
$\mathcal{O}(\alpha_{EM}^4\alpha_S^2)_{\text{TPI}}$	2.0×10^{-2} fb	3.0×10^{-3} fb	2.0×10^{-3} fb

Table 6: Cross sections for the processes which contribute to $W^+W^- + 2j$. For the second column the selection cuts are given in Eq.(5.1). For the third column the additional requirement Eq.(5.2) has been applied. The results in the last column also satisfy Eq.(5.3). In parentheses, in the fist row, are the cross sections obtained integrating the $8f$ contribution in the mass interval $118\,\text{GeV} \geq M_{WW} \geq 122\,\text{GeV}$ which corresponds in first approximation to the Higgs cross section.

Following Ref. [34] we then require the highest transverse momentum jet to be rather hard and a large separation in pseudorapidity between the most forward and most backward jets:

$$p_{T_{j1}} \geq 50 \text{ GeV}\,, \quad |\Delta\eta(j_f j_b)| > 4.2 \tag{5.2}$$

This leads to the results shown in the third column of Table 6. Finally we require that the two tag jets have a large invariant mass:

$$M_{jj} \geq 600\,\text{GeV}. \tag{5.3}$$

The corresponding cross sections are shown in the fourth column of Table 6. In parentheses, in the fist row of Table 6, are the cross sections obtained integrating the $8f$ contribution in the mass interval $118\,\text{GeV} \geq M_{WW} \geq 122\,\text{GeV}$ which corresponds in first approximation to the Higgs cross section.

The MPI background is modest to begin with, and is further reduced by the additional cuts Eq.(5.2) and Eq.(5.3), both in absolute terms and in the ratio to the Higgs signal, to a level at which it can be safely ignored.

6. Conclusions

In this paper we have estimated the contribution of Multiple Parton Interactions to $Z+4j$, $W^\pm W^\pm + 0/2j$ and $W^+W^- + 2j$ production.

The MPI contribution to $Z + 4j$ is dominated by events with two jets with balancing transverse momentum. It is possible to achieve a good signal to background ratio, close to 20%, for Multiple Interaction processes compared to Single Interaction ones by selecting events with two jets with large separation in the transverse plane and exploiting the expected resolution foreseen by both ATLAS and CMS in the polar angle ϕ. The corresponding statistical significance for a luminosity of 1 fb^{-1} is about 6.9 for the $\mu^+\mu^-$ channel alone with 260/1430 signal/background events. Comparisons with other reactions in which MPI processes can be measured should allow detailed studies of the flavour and fractional momentum dependence of Multiple Parton Interactions. Our preliminary analysis suggests that it might be possible to investigate TPI at the LHC using the $jj \otimes jj \otimes Z$ channel.

The $W^\pm W^\pm + 2j$ channel has a smaller rate. For a luminosity of 300 fb^{-1}, taking into account all possible decay channels to same–sign muons and electrons, the statistical significance of the MPI signal is 6.7 and the expected number of signal/background events is 280/1780 per experiment, with the basic selection cuts in Eq.(4.1) and Eq.(4.3).

The final state channel in which only two same–sign high transverse momentum charged leptons are required and additional hard jets are vetoed is dominated by MPI, with an expected rate of 2500 events with the full LHC luminosity. The SPI background amounts to about 20%. Provided the reducible background due to isolated lepton production in B-hadron decays can be kept under control, $W^\pm W^\pm + 0j$ provides a clean opportunity for studying Multiple Parton Interactions at the LHC.

Finally we have estimated the MPI background to $H \to WW \to \ell\ell\nu\nu$ production in the vector fusion channel and found it negligible.

Acknowledgments

This work has been supported by MIUR under contract 2006020509_004 and by the European Community's Marie-Curie Research Training Network under contract MRTN-CT-2006-035505 'Tools and Precision Calculations for Physics Discoveries at Colliders'

A. A loose argument for the relative size of the effective cross sections in Double and Triple Parton Interactions

An estimate of the relative size of the effective cross sections σ_{eff} and $\sigma_{3,eff}$ for DPI and TPI can be obtained as follows. Let us assume, being aware that this is a rather crude approximation, see Ref. [15, 16, 17], that the N–particle distribution function $\Gamma(x_1, b_1, ..., x_N, b_N)$ completely factorizes

$$\Gamma(x_1, b_1, ..., x_N, b_N) = \Gamma_1(x_1, b_1) \cdots \Gamma_N(x_N, b_N). \tag{A.1}$$

Let us also assume that the dependence of two particle distribution function on the momentum fraction x and on the transverse position b in turn factorize $\Gamma(x, b) = G(x)f(b)$ where G is the usual distribution function entering SPI and f is a universal function which does not depend on the nature of the parton.

We can then write the SPI cross section as:

$$\begin{aligned} \sigma_S &= \int G(x_1)\sigma_1(x_1, y_1)G(y_1)\, dx_1 dy_1 \\ &= \int G(x_1)f(b_1)\sigma_1(x_1, y_1)G(y_1)f(b_1 - \beta)\, dx_1\, dy_1\, d^2b_1\, d^2\beta \\ &= \sigma_1 \int T(\beta)\, d^2\beta \end{aligned} \tag{A.2}$$

where the overlap function $T = \int f(b)f(b-\beta)\, d^2b$ takes into account the dependence on the impact parameter β and on the parton distribution in the transverse plane. The overlap function, by definition, must be normalized to unity, $\int T(\beta)\, d^2\beta = 1$.

Analogously we can write the DPI cross section as follows:

$$\begin{aligned} \sigma_D &= \frac{1}{2!} \int G(x_1)f(b_1)\sigma_1(x_1, y_1)G(y_1)f(b_1 - \beta)\, dx_1\, dy_1\, d^2b_1 \\ &\qquad G(x_2)f(b_2)\sigma_2(x_2, y_2)G(y_2)f(b_2 - \beta)\, dx_2\, dy_2\, d^2b_2\, d^2\beta \\ &= \frac{1}{2!}\, \sigma_1\sigma_2 \int T^2(\beta)\, d^2\beta \\ &= \frac{1}{2!} \frac{\sigma_1\sigma_2}{\sigma_{2,eff}} \end{aligned} \tag{A.3}$$

and in general the N–Parton Interaction cross section can be expressed as:

$$\begin{aligned} \sigma_N &= \frac{1}{N!} \int G(x_1)f(b_1)\sigma_1(x_1, y_1)G(y_1)f(b_1 - \beta)\, dx_1\, dy_1\, d^2b_1 \\ &\qquad \cdots\cdots \\ &\qquad G(x_N)f(b_N)\sigma_N(x_N, y_N)G(y_N)f(b_N - \beta)\, dx_N\, dy_N\, d^2b_N\, d^2\beta \\ &= \frac{1}{N!}\, \sigma_1 \cdots \sigma_N \int T^N(\beta)\, d^2\beta \\ &= \frac{1}{N!} \frac{\sigma_1 \cdots \sigma_N}{\sigma_{N,eff}^{N-1}}. \end{aligned} \tag{A.4}$$

Therefore

$$\frac{1}{\sigma_{N,eff}^{N-1}} = \int T^N(\beta)\, d^2\beta. \tag{A.5}$$

To make progress we can assume for f a simple Gaussian model, which has been extensively considered in the literature,

$$f(b) = \frac{1}{2\pi\,\delta^2}\, e^{-b^2/(2\,\delta^2)}. \tag{A.6}$$

In this case

$$\int T^N(\beta)\, d^2\beta = \frac{1}{N}\, \frac{1}{(4\pi\,\delta^2)^{N-1}}\,. \tag{A.7}$$

Therefore the normalization condition is automatically satisfied and

$$\sigma_{2,eff} = \sigma_{eff} = 2\,(4\pi\,\delta^2) \qquad \sigma_{3,eff} = \sqrt{3}\,(4\pi\,\delta^2) \qquad \sigma_{N,eff} = N^{1/(N-1)}\,(4\pi\,\delta^2) \tag{A.8}$$

which indeed suggests that all $\sigma_{N,eff}$ are comparable to each other.

References

[1] T. Akesson *et al.* (Axial Field Spectrometer Collaboration), *Z. Phys.* **C34** (1987) 163.

[2] F. Abe *et al.* (CDF Collaboration),*Phys. Rev. Lett.* **79** (1997) 584, F. Abe *et al.* (CDF Collaboration), *Phys. Rev.* **D56** (1997) 3811

[3] The D0 Collaboration, D0 note 5910-CONF.

[4] T. Sjöstrand and P.Z. Skands, *JHEP* **03** (2004) 053, [hep-ph/0402078].

[5] T. Sjöstrand and P.Z. Skands, *Eur. Phys. J.* **C39** (2005) 129, [hep-ph/0408302].

[6] J.M. Butterworth, J.R. Forshaw and M.H. Seymour, *Z. Phys.* **C72** (1996) 637, [hep-ph/9601371].

[7] M. Bahr, S. Giesekeand M.H. Seymour, *JHEP* **07** (2008) 076, arXiv:0803.3633 [hep-ph].

[8] A. Del Fabbro and D. Treleani, *Phys. Rev.* **D61** (2000) 077502, [hep-ph/9911358].

[9] A. Del Fabbro and D. Treleani, *Phys. Rev.* **D66** (2002) 074012, [hep-ph/0207311].

[10] M.Y. Hussein, *Nucl. Phys. Proc. Supp.***B174**(2007)55, [hep-ph/0610207].

[11] S. Domdey, H.J. Pirner and U.A. Wiedemann, arXiv:0906.4335 [hep-ph].

[12] G. Calucci and D. Treleani, Phys. Rev.D79(2009)034002, arXiv:0809.4217 [hep-ph].

[13] G. Calucci and D. Treleani, Phys. Rev.D79(2009)074013, arXiv:0901.3089 [hep-ph].

[14] E. Maina, *JHEP* **04** (2009) 098, arXiv:0904.2682 [hep-ph].

[15] A.M. Snigirev, *Phys. Rev.* **D68** (2003) 114012, [hep-ph/0304172].

[16] V.L. Korotkikh and A.M. Snigirev, *Phys. Lett.* **B594** (2004) 171, [hep-ph/0404155].

[17] E. Cattaruzza, A. Del Fabbro and D. Treleani, *Phys. Rev.* **D72** (2005) 034022, [hep-ph/0507052].

[18] Z. Sullivan and E.L. Berger, *Phys. Rev.* **74** (2006) 033008, Z. Sullivan and E.L. Berger, *Phys. Rev.* **78** (2008) 034030.

[19] A. Kulesza and W.J. Stirling, *Phys. Lett.* **B475** (2000) 168.

[20] ATLAS Collaboration, *Detector and Physics Performance Technical Design Report*, Vols. 1 and 2, CERN–LHCC–99–14 and CERN–LHCC–99–15.

[21] CMS Collaboration,*Technical Design Report*, Vols. 1 and 2, CERN/LHCC 2006–001 and CERN/LHCC 2006–021.

[22] D. Treleani, *Phys. Rev.* **D76** (2007) 076006, arXiv:0708.2603 [hep-ph]

[23] A. Ballestrero, A. Belhouari, G. Bevilacqua, V. Kashkan and E. Maina, *Comp. Phys. Commun.* **180** (2009) 401, arXiv:0801.3359 [hep-ph]

[24] A. Ballestrero and E. Maina, *Phys. Lett.* **B350** (1995) 225, [hep-ph/9403244].

[25] A. Ballestrero, `PHACT 1.0` - *Program for Helicity Amplitudes Calculations with Tau matrices* [hep-ph/9911318] in *Proceedings of the 14th International Workshop on High Energy Physics and Quantum Field Theory (QFTHEP 99)*, B.B. Levchenko and V.I. Savrin eds. (SINP MSU Moscow), pg. 303.

[26] F. Maltoni, T. Stelzer, JHEP 0302 (2003) 027; T. Stelzer and W. F. Long, Comput. Phys. Commun. **81** (1994) 357; J. Alwall *et al.*, arXiv:0706.2334;
H. Murayama, I. Watanabe and K. Hagiwara, KEK-91-11.

[27] J. Alwall *et al.*, A Standard format for Les Houches event files. Written within the framework of the MC4LHC-06 workshop: Monte Carlos for the LHC: A Workshop on the Tools for LHC Event Simulation (MC4LHC), Geneva, Switzerland, 17-16 Jul 2005, *Comp. Phys. Commun.* **176** (2007) 300, [hep-ph/0609017].

[28] CTEQ Coll.(H.L. Lai *et al.*) *Eur. Phys. J.* **C12** (2000) 375.

[29] K.R. Ellis, K. Melnikov and G. Zanderighi, JHEP 04(2009)077, arXiv:0901.4101 [hep-ph];
K.R. Ellis, K. Melnikov and G. Zanderighi, arXiv:0906.1445 [hep-ph].

[30] C. FC. Berger, Z. Bern, L.J. Dixon, F. Febres Cordero, D. Forde, T. Gleisberg, H. Ita, D.A. Kosower and D. Maitre Phys. Rev. Lett. 102(2009)222001, arXiv:0902.2760 [hep-ph];
C. FC. Berger, Z. Bern, L.J. Dixon, F. Febres Cordero, D. Forde, T. Gleisberg, H. Ita, D.A. Kosower and D. Maitre arXiv:0907.1984 [hep-ph].

[31] See for instance the recent talks by R. Field http://www.phys.ufl.edu/∼rfield/

[32] S. Asai *et al.*, *Eur. Phys. J.* **C32 S2** (2004) 19.

[33] N. Amapane *et al.*, CMS Note AN 2007/005

[34] E. Yazgan *et al.*, CMS NOTE 2007/011.